nature portfolio

https://doi.org/10.1038/s41561-021-00693-5

Supplementary information

The future lifespan of Earth's oxygenated atmosphere

In the format provided by the authors and unedited

Supplementary Information for

The future lifespan of Earth's oxygenated atmosphere

Kazumi Ozaki* and Christopher T. Reinhard

*Corresponding author. E-mail: kazumi.ozaki@sci.toho-u.ac.jp

Supplementary Table 1. Mass balance equations.

Reservoir	Label	Differential equation
Marine phosphate	P	$\frac{dP}{dt} = J_{\mathrm{P}}^{\mathrm{riv}} - J_{\mathrm{P}}^{\mathrm{b}}$
Marine fixed nitrogen	N	$\frac{dN}{dt} = J_{\mathrm{Nfix}} - J_{\mathrm{deni}} - J_{\mathrm{Norg}}^{\mathrm{b}}$
†Atmosphere-ocean O_2	O	$\frac{dO}{dt} = \left(J_{\mathrm{NPP}}^{\mathrm{ocn}} - f_{\mathrm{O_2}} J_{\mathrm{org}}^{\mathrm{r,ocn}} - \delta f_{\mathrm{CH_4}} J_{\mathrm{org}}^{\mathrm{r,ocn}}\right) + \left(J_{\mathrm{NPP}}^{\mathrm{land}} - g_{\mathrm{O_2}} J_{\mathrm{org}}^{\mathrm{r,land}} - \delta g_{\mathrm{CH_4}} J_{\mathrm{org}}^{\mathrm{r,land}}\right)$ $- J_{\mathrm{org}}^{\mathrm{w}} - J_{\mathrm{org}}^{\mathrm{m}} + 2J_{\mathrm{py}}^{\mathrm{b}} - 2J_{\mathrm{py}}^{\mathrm{w}} - 2J_{\mathrm{CH_4ox}} - 0.5J_{\mathrm{Hesc}}^{\mathrm{CH_4}} + 0.5J_{\mathrm{Hesc}}^{\mathrm{H_2O}} - 2J_{\mathrm{H_2S}}^{\mathrm{d}} - J_{\mathrm{red}}^{\mathrm{d}} - 0.25J_{\mathrm{Fe\text{-}ox}}^{\mathrm{s}}$
†Atmosphere-ocean CO_2	A	$\frac{dA}{dt} = J_{\mathrm{CO_2}}^{\mathrm{d}} + J_{\mathrm{org}}^{\mathrm{w}} + J_{\mathrm{org}}^{\mathrm{m}} + J_{\mathrm{carb}}^{\mathrm{w}} + J_{\mathrm{carb}}^{\mathrm{m}} - J_{\mathrm{carb}}^{\mathrm{b}} + J_{\mathrm{CH_4ox}} + 0.5J_{\mathrm{Hesc}}^{\mathrm{CH_4}}$ $-\left(J_{\mathrm{NPP}}^{\mathrm{ocn}} - f_{\mathrm{O_2}} J_{\mathrm{org}}^{\mathrm{r,ocn}} - \frac{1+\delta}{2} f_{\mathrm{CH_4}} J_{\mathrm{org}}^{\mathrm{r,ocn}}\right) - \left(J_{\mathrm{NPP}}^{\mathrm{land}} - g_{\mathrm{O_2}} J_{\mathrm{org}}^{\mathrm{r,land}} - \frac{1+\delta}{2} g_{\mathrm{CH_4}} J_{\mathrm{org}}^{\mathrm{r,land}}\right)$
†Atmospheric CH_4	M	$\frac{dM}{dt} = (1-\delta)0.5 f_{\mathrm{CH_4}} J_{\mathrm{org}}^{\mathrm{r,ocn}} + (1-\delta)0.5 g_{\mathrm{CH_4}} J_{\mathrm{org}}^{\mathrm{r,land}} - J_{\mathrm{CH_4ox}} - 0.5J_{\mathrm{Hesc}}^{\mathrm{CH_4}}$
†Ocean alkalinity	ALK	$\frac{dALK}{dt} = 2\left(J_{\mathrm{sil}}^{\mathrm{w}} + J_{\mathrm{carb}}^{\mathrm{w}} - J_{\mathrm{carb}}^{\mathrm{b}}\right)$
Ocean calcium ion	CAL	$\frac{dCAL}{dt} = J_{\mathrm{sil}}^{\mathrm{w}} + J_{\mathrm{carb}}^{\mathrm{w}} + J_{\mathrm{gyp}}^{\mathrm{w}} - J_{\mathrm{carb}}^{\mathrm{b}} - J_{\mathrm{gyp}}^{\mathrm{b}}$
†Sedimentary organic C	G	$\frac{dG}{dt} = J_{\mathrm{org}}^{\mathrm{b,ocn}} + J_{\mathrm{org}}^{\mathrm{b,land}} - J_{\mathrm{org}}^{\mathrm{w}} - J_{\mathrm{org}}^{\mathrm{m}} - J_{\mathrm{org}}^{\mathrm{s}}$
†Sedimentary carbonate C	C	$\frac{dC}{dt} = J_{\mathrm{carb}}^{\mathrm{b}} - J_{\mathrm{carb}}^{\mathrm{w}} - J_{\mathrm{carb}}^{\mathrm{m}} - J_{\mathrm{carb}}^{\mathrm{s}}$
†Ocean sulphate	S	$\frac{dS}{dt} = J_{\mathrm{H_2S}}^{\mathrm{d}} + J_{\mathrm{gyp}}^{\mathrm{w}} + J_{\mathrm{py}}^{\mathrm{w}} - J_{\mathrm{gyp}}^{\mathrm{b}} - J_{\mathrm{py}}^{\mathrm{b}}$
†Sedimentary pyrite S	PYR	$\frac{dPYR}{dt} = J_{\mathrm{py}}^{\mathrm{b}} - J_{\mathrm{py}}^{\mathrm{w}} - J_{\mathrm{py}}^{\mathrm{s}}$
†Sedimentary gypsum S	GYP	$\frac{dGYP}{dt} = J_{\mathrm{gyp}}^{\mathrm{b}} - J_{\mathrm{gyp}}^{\mathrm{w}} - J_{\mathrm{gyp}}^{\mathrm{s}}$

† denotes equations that is altered from the original model[1].

Supplementary Table 2 Parameter values used in this study.

Parameter	Label	Value	Unit	Ref.
Reservoir size				
Reference value of marine phosphate inventory	P^*	3.1	$\times 10^{15}$ mol P	[1]
Reference value of marine nitrate inventory	N^*	43.5	$\times 10^{15}$ mol N	[1]
Reference value of O_2 in the ocean-atmosphere system	O^*	37	$\times 10^{18}$ mol O_2	[1]
Reference value of inorganic C in the ocean-atmosphere system	A^*	3.193	$\times 10^{18}$ mol C	[1]
Reference value of crustal organic C reservoir size	G^*	1250	$\times 10^{18}$ mol C	[1]
Reference value of crustal carbonate C reservoir size	C^*	5000	$\times 10^{18}$ mol C	[1]
Reference value of marine sulphate reservoir size	S^*	40	$\times 10^{18}$ mol S	[1]
Reference value of crustal pyrite S reservoir size	PYR^*	180	$\times 10^{18}$ mol S	[1]
Reference value of crustal gypsum S reservoir size	GYP^*	200	$\times 10^{18}$ mol S	[1]
Reference value of marine calcium ion reservoir size	CAL^*	13.97	$\times 10^{18}$ mol Ca	[1]
Reference value of marine alkalinity reservoir size	ALK^*	3.2	$\times 10^{18}$ eq	This study
Atmospheric composition				
Reference value of atmospheric CO_2 mixing ratio	fCO_2^*	280	ppmv	[1]
Reference value of atmospheric O_2 level	p_{O2}^*	0.21	atm	[1]
Reference value of atmospheric CH_4 mixing ratio	fCH_4^*	0.715	ppmv	[2]
Biogeochemical flux				
Reference value of CO_2 outgassing via metamorphism of organic C	$J_{org}^{m,*}$	1.25	Tmol C yr^{-1}	[1]
Reference value of continental silicate weathering	$J_{sil}^{w,*}$	6.65	Tmol yr^{-1}	[1]
Reference value of continental carbonate weathering	$J_{carb}^{w,*}$	13.35	Tmol yr^{-1}	[1]
Reference value of gypsum weathering	$J_{gyp}^{w,*}$	1.0	Tmol S yr^{-1}	[1]
Reference value of subduction flux of gypsum S	$J_{gyp}^{s,*}$	0.0	Tmol S yr^{-1}	This study
Reference value of pyrite weathering	$J_{pyr}^{w,*}$	0.53	Tmol S yr^{-1}	[1]
Reference value of burial rate of terrigenous organic C	$J_{org}^{b,land*}$	4.5	Tmol C yr^{-1}	[1]
Reference value of nitrogen fixation	J_{nfix}^{*}	8.72	Tmol N yr^{-1}	[1]
Reference value of denitrification	J_{deni}^{*}	8.60	Tmol N yr^{-1}	[1]
Reference value of burial rate of marine organic C	$J_{org}^{b,ocn*}$	4.5	Tmol C yr^{-1}	[1]
Reference value of P weathering	$J_{P}^{w,*}$	0.0435	Tmol P yr^{-1}	[1]
Reference value of burial rate of Fe-bound P	$J_{Fe\text{-}P}^{b,*}$	0.006	Tmol P yr^{-1}	[3]
Reference value of burial rate of authigenic P	$J_{authP}^{b,*}$	0.015	Tmol P yr^{-1}	[3]
Reference value of CH_4 efflux from terrestrial biosphere†	$J_{CH4}^{land,*}$	1.0	Tmol CH_4 yr^{-1}	This study
Reference value of marine new production	J_{NP}^{ocn*}	225.96	μmol C kg^{-1}	[3]
Reference value of net primary production of oceanic ecosystem	J_{NPP}^{ocn*}	3750	Tmol C yr^{-1}	[4]
Reference value of net primary production of terrestrial ecosystem	J_{NPP}^{land*}	5000	Tmol C yr^{-1}	[4]

(Continued on the next page)

Supplementary Table 2 (continued)

Parameter	Label	Value	Unit	Ref.
Other parameters				
Present value of solar constant	$S_{\odot}{}^{0}$	1368	W m^{-2}	5
Age of the Earth	τ	4.55	10^9 yr	5
Reference value of surface temperature	$T_C{}^{*}$	15	℃	1
Optimum temperature for marine productivity	T_{opt}	28	℃	6
Temperature factor for marine productivity	ΔT_{opt}	28	℃	6
Temperature threshold for global glaciation	T_{ice}	263	K	This study
Temperature threshold for ice free conditions	T_0	273	K	This study
Ice albedo	α_{ice}	0.65		This study
Albedo for warm climatic condition	α_{00}	0.35		This study
z: zenith angle	$\mu = \cos(z)$	0.6		This study
Hydrogen escape factor	f_{esc}	6.6845	$\times 10^{15}$ mol yr^{-1}	This study
Mass of the ocean	M_{ocn}	1.476	$\times 10^{21}$ kg	This study
Oceanic volume	V_{ocn}	1.38	$\times 10^{18}$ m^3	This study
Seawater density	ρ	1025	kg m^{-3}	This study
Seawater salinity	*sal*	35	‰	This study
Fire frequency constant	k_{fire}	3		7
Runoff factor for carbonate weathering	RUN_{carb}	0.087		1
Temperature factor for the terrestrial CH_4 flux	a_{CH4}	1/11.07		8
Temperature factor for the terrestrial CH_4 flux	b_{CH4}	2.4		8
Reference value of oceanic anoxic fraction	DOA^{*}	0.14		3
Half-saturation constant for aerobic respiration	K_{O2}	13.6	$\times 10^{18}$ mol	9
Half-saturation constant for methanotrophy	$K_{O2}{}^{'}$	0.273	$\times 10^{18}$ mol	9
Proportional constant for carbonate precipitation	k_{carb}	3	Tmol yr^{-1}	This study
Exponential factor for carbonate precipitation	n_{cal}	1.7		10
C_{org}/P_{org} stoichiometry of primary producers	$r_{C/P}$	117	mol mol^{-1}	1
N_{org}/P_{org} stoichiometry of primary producers	$r_{N/P}$	16	mol mol^{-1}	1
Reference value of C_{org}/P_{org} stoichiometry of terrigenous organic C	$(C_{org}/P_{org})_{bur}{}^{land,*}$	1000	mol mol^{-1}	11
Reference value of C_{org}/N_{org} of buried sediments	$(C_{org}/N_{org})_{bur}{}^{*}$	37.5	mol mol^{-1}	3
C_{org}/P_{org} ratio of buried oxic sediments	$(C_{org}/P_{org})_{oxic}$	217	mol mol^{-1}	3

†Based on the photochemical parameterization (Supplementary Tables 3 and 4).

Supplementary Table 3. Functional forms.

Process	Function	Unit	Ref.
Climate			
Solar constant	$S_{\odot} = S_{\odot}^{0}\left(1-0.38t/\tau\right)^{-1}$	W m^{-2}	5
Surface albedo	$\alpha_{\mathrm{s}} = \begin{cases} \alpha_{00} & (T_0 \le T_{\mathrm{s}}) \\ \alpha_{\mathrm{ice}} - \left(\alpha_{\mathrm{ice}} - \alpha_{00}\right)\dfrac{\left(T_{\mathrm{s}} - T_{\mathrm{ice}}\right)^2}{\left(T_0 - T_{\mathrm{ice}}\right)^2} & (T_{\mathrm{ice}} \le T_{\mathrm{s}} \le T_0) \\ \alpha_{\mathrm{ice}} & (T_{\mathrm{s}} \le T_{\mathrm{ice}}) \end{cases}$		This study
Albedo of the top of atmosphere	$\alpha = z_1 + z_2\alpha_{\mathrm{s}} + z_3T_{\mathrm{s}} + z_4p + z_5\mu + z_6\alpha_{\mathrm{s}}p + z_7\mu p + z_8\alpha_{\mathrm{s}}\mu + z_9\alpha_{\mathrm{s}}T_{\mathrm{s}} + z_{10}\mu T_{\mathrm{s}} + z_{11}pT_{\mathrm{s}} + z_{12}\alpha_{\mathrm{s}}^{\,2} + z_{13}T_{\mathrm{s}}^{\,2} + z_{14}p^2 + z_{15}\mu^2$ $p = p_{\mathrm{CO_2}}$ (in bar) (190K $< T_{\mathrm{s}} <$ 280K) z_1 = -0.68910, z_2 = 1.0460, z_3 = 0.0078054, z_4 = -0.0028373, z_5 = -0.28899, z_6 = -0.037412, z_7 = -0.0063499, z_8 = 0.20122, z_9 = -0.0018508, $z_{10} = 1.3649\times10^{-4}$, $z_{11} = 9.8581\times10^{-5}$, z_{12} = 0.073239, $z_{13} = -1.6555\times10^{-5}$, $z_{14} = 6.5817\times10^{-4}$, z_{15} = 0.081218 (280K $< T_{\mathrm{s}} <$ 370K) z_1 = 1.1082, z_2 = 1.5172, z_3 = -0.0057993, z_4 = 0.019705, z_5 = -0.1867, z_6 = -0.031355, z_7 = -0.010214, z_8 = 0.20986, z_9 = -0.0037098, $z_{10} = -1.1335\times10^{-4}$, $z_{11} = 5.3714\times10^{-5}$, z_{12} = 0.075887, $z_{13} = 9.269\times10^{-6}$, $z_{14} = -4.1327\times10^{-4}$, z_{15} = 0.063298		12
Outgoing longwave radiation	$J_{\mathrm{OLR}} = x_1 + x_2\phi + x_3T_{\mathrm{s}} + x_4\phi T_{\mathrm{s}} + x_5\phi^2 + x_6T_{\mathrm{s}}^{\,2} + x_7\phi^2T_{\mathrm{s}} + x_8\phi T_{\mathrm{s}}^{\,2} + x_9\phi^2T_{\mathrm{s}}^{\,2} + x_{10}\phi^3 + x_{11}T_{\mathrm{s}}^{\,3} + x_{12}\phi^3T_{\mathrm{s}} + x_{13}\phi^3T_{\mathrm{s}}^{\,2} + x_{14}\phi T_{\mathrm{s}}^{\,3} + x_{15}\phi^2T_{\mathrm{s}}^{\,3} + x_{16}\phi^3T_{\mathrm{s}}^{\,3} + x_{17}\phi^4 + x_{18}\phi^4T_{\mathrm{s}} + x_{19}\phi^4T_{\mathrm{s}}^{\,2} + x_{20}\phi^4T_{\mathrm{s}}^{\,3}$ $\phi = \ln\dfrac{p_{\mathrm{CO_2}}\ (\text{in bar})}{3.3\times10^{-4}}$	W m^{-2}	12

(Continued on the next page)

Supplementary Table 3 (continued)

Process	Function	Unit	Ref.
	$(190\text{K} < T_s < 380\text{K})$ $x_1 = 9.46898,\ x_2 = -7.714727\times10^{-5},\ x_3 = -2.794778,\ x_4 = -3.244753\times10^{-3},$ $x_5 = -3.547406\times10^{-4},\ x_6 = 0.02212108,\ x_7 = 2.229142\times10^{-3},\ x_8 = 3.088497\times10^{-5},$ $x_9 = -2.789815\times10^{-5},\ x_{10} = -3.442973\times10^{-3},\ x_{11} = -3.361939\times10^{-5},\ x_{12} = 9.173169\times10^{-3},$ $x_{13} = -7.775195\times10^{-5},\ x_{14} = -1.679112\times10^{-7},\ x_{15} = 6.590999\times10^{-8},\ x_{16} = 1.528125\times10^{-7},$ $x_{17} = -0.03367567,\ x_{18} = -1.631909\times10^{-4},\ x_{19} = 3.663871\times10^{-6},\ x_{20} = -9.255646\times10^{-9}$		
Radiative forcing of CH_4	$RF_{\mathrm{CH_4}} = \begin{cases} m_1\left(\sqrt{f\mathrm{CH_4}} - \sqrt{0.715\times10^{-6}}\right) - m_2\left(\sqrt{f\mathrm{CH_4}} - \sqrt{0.715\times10^{-6}}\right)^2 \\ m_3 + m_4\log\left(\frac{f\mathrm{CH_4}}{2.5\times10^{-6}}\right) + m_5\left(\log\left(\frac{f\mathrm{CH_4}}{2.5\times10^{-6}}\right)\right)^2 \end{cases}$ $m_1 = 1173,\ m_2 = 71636,\ m_3 = 0.824,\ m_4 = 0.8,\ m_5 = 0.2$	W m^{-2}	2
Energy balance equation	$(1\text{-}\alpha)\frac{S_\odot}{4} = J_{\mathrm{OLR}} - RF_{\mathrm{CH_4}}$		This study
Photochemistry			
CH_4 oxidation	$J_{\mathrm{CH_4ox}} = k_{\mathrm{CH_4ox}} \times O \times M$	mol CH_4 yr^{-1}	6
	$\log k_{\mathrm{CH_4ox}} = \alpha_0^j + \alpha_1^j\varphi_{\mathrm{O_2}} + \alpha_2^j\varphi_{\mathrm{O_2}}{}^2 + \alpha_3^j\varphi_{\mathrm{O_2}}{}^3 + \alpha_4^j\varphi_{\mathrm{O_2}}{}^4 + \alpha_5^j\varphi_{\mathrm{O_2}}{}^5 + \alpha_6^j\varphi_{\mathrm{O_2}}{}^6$		This study
	$\varphi_{\mathrm{O_2}} = \log p_{\mathrm{O_2}}$		This study
Hydrogen escape	$J_{\mathrm{Hesc}} = f_{\mathrm{esc}} \cdot f_{\mathrm{T}}(\mathrm{H_2}) = J_{\mathrm{Hesc}}^{\mathrm{H_2O}} + J_{\mathrm{Hesc}}^{\mathrm{CH_4}}$	mol H_2 yr^{-1}	
	$f_{\mathrm{T}}(\mathrm{H_2}) = f\mathrm{H_2O} + 2f\mathrm{CH_4}$		This study
	$J_{\mathrm{Hesc}}^{\mathrm{H_2O}} = f_{\mathrm{esc}} f\mathrm{H_2O}$	mol H_2 yr^{-1}	
	$J_{\mathrm{Hesc}}^{\mathrm{CH_4}} = 2 f_{\mathrm{esc}} f\mathrm{CH_4}$	mol H_2 yr^{-1}	
	$\log_{10} f\mathrm{H_2O} = f_0 + f_1 T_s + f_2 T_s^2 + f_3 T_s^3$		13
	$f_0 = 198.34,\ f_1 = -1.6856,\ f_2 = 4.147\times10^{-3},\ f_3 = -2.7947\times10^{-6}$		

(Continued on the next page)

Supplementary Table 3 (continued)

Process	Function	Unit	Ref.
Degassing			
CO_2 degassing flux via metamorphism of sedimentary carbonates	$J^{\mathrm{m}}_{\mathrm{carb}} = f_{\mathrm{G}} f_{\mathrm{C}} \left(\frac{C}{C^*} \right) J^{\mathrm{m},*}_{\mathrm{carb}}$	mol C yr^{-1}	1
CO_2 degassing flux via metamorphism of sedimentary organic C	$J^{\mathrm{m}}_{\mathrm{org}} = f_{\mathrm{G}} \left(\frac{G}{G^*} \right) J^{\mathrm{m},*}_{\mathrm{org}}$	mol C yr^{-1}	1
CO_2 degassing flux from the mantle	$J^{\mathrm{d}}_{\mathrm{CO_2}} = f_{\mathrm{G}} J^{\mathrm{d},*}_{\mathrm{CO_2}}$	mol C yr^{-1}	This study
H_2S degassing flux from the mantle	$J^{\mathrm{d}}_{\mathrm{H_2S}} = f_{\mathrm{G}} J^{\mathrm{d},*}_{\mathrm{H_2S}}$	mol S yr^{-1}	This study
Reductant input flux from the mantle	$J^{\mathrm{d}}_{\mathrm{red}} = f_{\mathrm{G}} J^{\mathrm{d},*}_{\mathrm{red}}$	mol O_2 equiv. yr^{-1}	This study
Weathering/Riverine flux			
Silicate weathering	$J^{\mathrm{w}}_{\mathrm{sil}} = f_{\mathrm{R}} f_{\mathrm{CO_2}} \left(LIFE + (1 - LIFE) f_{\mathrm{E}} V \right) J^{\mathrm{w},*}_{\mathrm{sil}}$ $f_{\mathrm{CO_2}} = f_{\mathrm{pre}}(1 - mvw) + f_{\mathrm{post}} mvw$ $f_{\mathrm{pre}} = f_{\mathrm{T}} R_{\mathrm{CO_2}}{}^{0.5}$ $f_{\mathrm{post}} = f_{\mathrm{T}} \left(\frac{2R_{\mathrm{CO_2}}}{1 + R_{\mathrm{CO_2}}} \right)^{FERT}$ $R_{\mathrm{CO_2}} = \frac{p_{\mathrm{CO_2}}}{p^*_{\mathrm{CO_2}}}$ $f_{\mathrm{T}} = \exp\left(ACT(T_{\mathrm{C}} - T^*_{\mathrm{C}}) \right) \times \left(1 + RUN_{\mathrm{sil}}(T_{\mathrm{C}} - T^*_{\mathrm{C}}) \right)^{0.65}$ $mvw = V \times f_{\mathrm{E}}$	mol yr^{-1}	1

(Continued on the next page)

Supplementary Table 3 (continued)

Process	Function	Unit	Ref.
Carbonate weathering			
	$J^{\mathrm{w}}_{\mathrm{carb}} = f_{\mathrm{R}} g_{\mathrm{CO_2}} \left(LIFE + (1-LIFE) f_{\mathrm{E}} V \right) J^{\mathrm{w,*}}_{\mathrm{carb}}$	mol yr^{-1}	[1]
	$g_{\mathrm{CO_2}} = g_{\mathrm{pre}} (1 - mvw) + g_{\mathrm{post}} mvw$		
	$g_{\mathrm{pre}} = g_{\mathrm{T}} {R_{\mathrm{CO_2}}}^{0.5}$		
	$g_{\mathrm{post}} = g_{\mathrm{T}} \left(\frac{2R_{\mathrm{CO_2}}}{1+R_{\mathrm{CO_2}}} \right)^{FERT}$		
	$g_{\mathrm{T}} = 1 + RUN_{\mathrm{carb}} \left(T_{\mathrm{C}} - T^{*}_{\mathrm{C}} \right)$		
Oxidative weathering of sedimentary organic C			
	$J^{\mathrm{w}}_{\mathrm{org}} = f_{\mathrm{R}} \left(\frac{G}{G^{*}} \right) \left(\frac{O}{O^{*}} \right)^{0.5} J^{\mathrm{w,*}}_{\mathrm{org}}$	mol C yr^{-1}	[1]
	$J^{\mathrm{w,*}}_{\mathrm{org}} = J^{\mathrm{b,ocn,*}}_{\mathrm{org}} + J^{\mathrm{b,land,*}}_{\mathrm{org}} - J^{\mathrm{m,*}}_{\mathrm{org}} - J^{\mathrm{s,*}}_{\mathrm{org}}$	mol C yr^{-1}	This study
Gypsum weathering			
	$J^{\mathrm{w}}_{\mathrm{gyp}} = \left(\frac{GYP}{GYP^{*}} \right) \frac{J^{\mathrm{w}}_{\mathrm{carb}}}{J^{\mathrm{w*}}_{\mathrm{carb}}} J^{\mathrm{w,*}}_{\mathrm{gyp}}$	mol S yr^{-1}	[1]
Oxidative weathering of sedimentary pyrite S			
	$J^{\mathrm{w}}_{\mathrm{py}} = f_{\mathrm{R}} \left(\frac{PYR}{PYR^{*}} \right) \left(\frac{O}{O^{*}} \right)^{0.5} J^{\mathrm{w,*}}_{\mathrm{py}}$	mol S yr^{-1}	[1]
Phosphorus weathering			
	$J^{\mathrm{w}}_{\mathrm{P}} = f_{\mathrm{pP}} \left(\frac{2}{12} \frac{J^{\mathrm{w}}_{\mathrm{sil}}}{J^{\mathrm{w*}}_{\mathrm{sil}}} + \frac{5}{12} \frac{J^{\mathrm{w}}_{\mathrm{carb}}}{J^{\mathrm{w*}}_{\mathrm{carb}}} + \frac{5}{12} \frac{J^{\mathrm{w}}_{\mathrm{orgC}}}{J^{\mathrm{w*}}_{\mathrm{orgC}}} \right) J^{\mathrm{w,*}}_{\mathrm{P}}$	mol P yr^{-1}	[1]
P flux to the terrestrial ecosystem			
	$J^{\mathrm{land}}_{\mathrm{P}} = k_{11} \times V \times J^{\mathrm{w,*}}_{\mathrm{P}}$	mol P yr^{-1}	[1]
Riverine P flux to the ocean			
	$J^{\mathrm{riv}}_{\mathrm{P}} = \left(1 - k_{11} V \right) J^{\mathrm{w,*}}_{\mathrm{P}}$	mol P yr^{-1}	[1]

(Continued on the next page)

Supplementary Table 3 (continued)

Process	Function	Unit	Ref.
Land biosphere			
NPP of terrestrial biosphere			
	$J_{\mathrm{NPP}}^{\mathrm{land}} = V \times J_{\mathrm{NPP}}^{\mathrm{land},*}$	Gt C yr^{-1}	This study
Activity level of terrestrial biosphere			
	$V = f_{\mathrm{UV}} f_{\mathrm{P}} f_{\mathrm{fire}} V_{\mathrm{npp}}$	Present Level	This study
	$V_{\mathrm{npp}} = 2 \times V_{\mathrm{O_2}} \times V_{\mathrm{CO_2}} \times V_T$		1
	$V_{\mathrm{T}} = \begin{cases} 1-\left(\dfrac{T_{\mathrm{C}}-25}{25}\right)^2 & \left(T_{\mathrm{C}} < 25\ ^{\circ}\mathrm{C}\right) \\ 1-\left(\dfrac{T_{\mathrm{C}}-25}{T_{\mathrm{ref}}^{\mathrm{land}}}\right)^2 & \left(T_{\mathrm{C}} \geq 25\ ^{\circ}\mathrm{C}\right) \end{cases}$		1
	$V_{\mathrm{CO_2}} = \dfrac{p_{\mathrm{CO_2}} - P_{\mathrm{min}}}{K_{\mathrm{P}} + p_{\mathrm{CO_2}} - P_{\mathrm{min}}}$		1
	$K_{\mathrm{P}} = \left(2V_T^* - 1\right)\left(p_{\mathrm{CO_2}}^* - P_{\mathrm{min}}\right)$		
	$V_{\mathrm{O_2}} = 1.5 - 0.5\left(\dfrac{O}{O^*}\right)$		1
	$f_{\mathrm{fire}} = \dfrac{k_{\mathrm{fire}}}{k_{\mathrm{fire}} - 1 + ignit}$		1
	$f_{\mathrm{UV}} = \tanh\left(\dfrac{p_{\mathrm{O_2}}^{\mathrm{PAL}}}{c_{\mathrm{UV}}}\right)$		This study
	$ignit = \min\left\{\max\left\{48\,f\mathrm{O_2} - 9.08, 0\right\}, 5\right\}$		14
Burial rate of terrigenous organic C			
	$J_{\mathrm{org}}^{\mathrm{b,land}} = \left(\mathrm{C_{org}}/\mathrm{P_{org}}\right)_{\mathrm{bur}}^{\mathrm{land}} J_{\mathrm{P}}^{\mathrm{land}}$	mol C yr^{-1}	1
CH_4 efflux from the terrestrial biosphere to the atmosphere			
	$J_{\mathrm{CH_4}}^{\mathrm{land}} = \left(\dfrac{J_{\mathrm{orgC}}^{\mathrm{b,land}}}{J_{\mathrm{orgC}}^{\mathrm{b,land},*}}\right) f_T^{\mathrm{land}} J_{\mathrm{CH_4}}^{\mathrm{land},*}$	mol yr^{-1}	This study

(Continued on the next page)

Supplementary Table 3 (continued)

Process	Function	Unit	Ref.
	$f_T^{\text{land}} = a_{\text{CH}_4} \exp\left(b_{\text{CH}_4} T_{\text{C}} / T_{\text{C}}^*\right)$		8
Fraction of methanogenesis			
	$g_{\text{CH}_4} = \dfrac{J_{\text{CH}_4}^{\text{land}}}{(1-\delta) J^{\text{r,land}} / 2}$		This study
Fraction of aerobic respiration			
	$g_{\text{O}_2} = 1 - g_{\text{CH}_4}$		This study
Marine biosphere			
NPP of marine biosphere			
	$J_{\text{NPP}}^{\text{ocn}} = \left(\dfrac{J_{\text{NP}}^{\text{ocn}}}{J_{\text{NP}}^{\text{ocn*}}}\right) J_{\text{NPP}}^{\text{ocn,*}}$	Gt C yr^{-1}	This study
New production of marine biosphere			
	$J_{\text{NP}}^{\text{ocn}} = f_n f_T^{\text{ocn}} J_{\text{NP}}^{\text{ocn*}}$	μmol C kg^{-1}	This study
	$f_n = \dfrac{Minimum\left[r_{\text{C/N}} N, r_{\text{C/P}} P, M_{\text{CO}_2+\text{HCO}_3^-}\right]}{r_{\text{C/N}} N^*}$		This study
	$f_T^{\text{ocn}}(T_{\text{s}}) = \begin{cases} 0 & \left(T_{\text{s}} < 273\ \text{K}\right) \\ k\left\{1 - \left(\dfrac{T_{\text{opt}} - T_{\text{s}}}{\Delta T_{\text{opt}}}\right)^2\right\} & \left(273\ \text{K} \le T_{\text{s}} \le 301\ \text{K}\right) \\ k\left[\left\{1 - \left(\dfrac{T_{\text{opt}} - T_{\text{s}}}{\Delta T_{\text{opt}}}\right)^2\right\} \exp\left(-\dfrac{\left\lvert T_{\text{s}} - T_{\text{opt}}\right\rvert^3}{T_{\text{ref}}}\right)\right] & \left(T_{\text{s}} \ge 301\ \text{K}\right) \end{cases}$		6
Degree of anoxia			
	$DOA = 1 - \left(1 - DOA^*\right)\left(\dfrac{O}{O^*}\right)\left(\dfrac{J_{\text{NP}}^{\text{ocn*}}}{J_{\text{NP}}^{\text{ocn}}}\right)$		3

(Continued on the next page)

Supplementary Table 3 (continued)

Process	Function	Unit	Ref.
Nitrogen fixation	$J_{\mathrm{Nfix}} = J^{*}_{\mathrm{Nfix}} \left(\frac{P - N/r_{\mathrm{N/P}}}{P^{*} - N^{*}/r_{\mathrm{N/P}}} \right)^{2}$	mol N yr^{-1}	3
Denitrification	$J_{\mathrm{deni}} = J^{*}_{\mathrm{deni}} \left(1 + \frac{DOA}{DOA^{*}} \right) 0.5$	mol N yr^{-1}	3
Fraction of aerobic respiration	$f_{\mathrm{O_2}} = \frac{O}{O + K_{\mathrm{O_2}}}$		9
Fraction of methanogenesis	$f_{\mathrm{CH_4}} = 1 - f_{\mathrm{O_2}}$		9
Fraction of methane consumed by methanotrophy	$\delta = \frac{O}{O + K_{\mathrm{O_2}}'}$		9
Burial rate of organic C in marine sediments	$J^{\mathrm{b,ocn}}_{\mathrm{org}} = J^{\mathrm{b,ocn*}}_{\mathrm{org}} \left(\frac{J^{\mathrm{ocn}}_{\mathrm{NP}}}{J^{\mathrm{ocn*}}_{\mathrm{NP}}} \right)^{2}$	mol C yr^{-1}	3
Burial rate of organic N in marine sediments	$J^{\mathrm{b,ocn}}_{\mathrm{Norg}} = \frac{J^{\mathrm{b,ocn}}_{\mathrm{org}}}{\left(\mathrm{C_{org}}/\mathrm{N_{org}} \right)_{\mathrm{bur}}}$	mol N yr^{-1}	3
Burial rate of reactive P in marine sediments	$J^{\mathrm{b}}_{\mathrm{P}} = J^{\mathrm{b}}_{\mathrm{Porg}} + J^{\mathrm{b}}_{\mathrm{Fe\text{-}P}} + J^{\mathrm{b}}_{\mathrm{Pauth}}$ $J^{\mathrm{b}}_{\mathrm{Porg}} = \frac{J^{\mathrm{b,ocn}}_{\mathrm{org}}}{\left(\mathrm{C_{org}}/\mathrm{P_{org}} \right)_{\mathrm{bur}}}$ (Organic P burial) $J^{\mathrm{b}}_{\mathrm{Fe\text{-}P}} = J^{\mathrm{b,*}}_{\mathrm{Fe\text{-}P}} \left(\frac{1 - DOA}{1 - DOA^{*}} \right)$ (Iron-bound P burial) $J^{\mathrm{b}}_{\mathrm{Pauth}} = J^{\mathrm{b,*}}_{\mathrm{Pauth}} \left(\frac{J^{\mathrm{ocn}}_{\mathrm{NP}}}{J^{\mathrm{ocn*}}_{\mathrm{NP}}} \right)^{2}$ (Authigenic P burial)	mol P yr^{-1}	3

(Continued on the next page)

Supplementary Table 3 (continued)

Process	Function	Unit	Ref.
	$\left(\mathrm{C_{org}}/\mathrm{P_{org}}\right)_{\mathrm{bur}} = \dfrac{\left(\mathrm{C_{org}}/\mathrm{P_{org}}\right)_{\mathrm{oxic}}\left(\mathrm{C_{org}}/\mathrm{P_{org}}\right)_{\mathrm{anoxic}}}{(1-DOA)\left(\mathrm{C_{org}}/\mathrm{P_{org}}\right)_{\mathrm{anoxic}} + DOA\left(\mathrm{C_{org}}/\mathrm{P_{org}}\right)_{\mathrm{oxic}}}$		3
Pyrite burial			
	$J_{\mathrm{py}}^{\mathrm{b}} = J_{\mathrm{py}}^{\mathrm{b},*}\left(\dfrac{S}{S^*}\right)\left(\dfrac{J_{\mathrm{org}}^{\mathrm{b}}}{J_{\mathrm{org}}^{\mathrm{b},*}}\right)\left(\dfrac{O^*}{O}\right)$	mol S yr^{-1}	1
	$J_{\mathrm{py}}^{\mathrm{b},*} = J_{\mathrm{py}}^{\mathrm{w},*} + J_{\mathrm{py}}^{\mathrm{s},*}$	mol S yr^{-1}	This study
Gypsum deposition			
	$J_{\mathrm{gyp}}^{\mathrm{b}} = J_{\mathrm{gyp}}^{\mathrm{b},*}\left(\dfrac{S}{S^*}\right)\left(\dfrac{CAL}{CAL^*}\right)$	mol S yr^{-1}	1
	$J_{\mathrm{gyp}}^{\mathrm{b},*} = J_{\mathrm{gyp}}^{\mathrm{w},*} + J_{\mathrm{gyp}}^{\mathrm{s},*}$	mol S yr^{-1}	This study
Carbonate precipitation			
	$J_{\mathrm{carb}}^{\mathrm{b}} = k_{\mathrm{carb}}\left(\Omega - 1\right)^{n_{\mathrm{cal}}}$	mol C yr^{-1}	10
	$\Omega = \dfrac{[\mathrm{Ca}^{2+}][\mathrm{CO_3^{2-}}]}{K_{\mathrm{sp}}}$		
	$[\mathrm{Ca}^{2+}] = CAL/M_{\mathrm{ocn}}$	mol kg^{-1}	
	$[\mathrm{CO_3^{2-}}] = \dfrac{ALK/M_{\mathrm{ocn}}}{2 + [\mathrm{H^+}]/K_2}$	mol kg^{-1}	
	$[\mathrm{HCO_3^-}] = \dfrac{[\mathrm{CO_3^{2-}}][\mathrm{H^+}]}{K_2}$	mol kg^{-1}	
	$[\mathrm{CO_2}]_{\mathrm{aq}} = \dfrac{[\mathrm{CO_3^{2-}}][\mathrm{H^+}]^2}{K_1 K_2}$	mol kg^{-1}	
	$p_{\mathrm{CO_2}} = \dfrac{[\mathrm{CO_2}]_{\mathrm{aq}}}{K_0}$	atm	
	$\ln K_0 = a_0 + a_1\left(\dfrac{100}{T_{\mathrm{s}}}\right) + a_2 \ln\left(\dfrac{100}{T_{\mathrm{s}}}\right) + sal\left(a_3 + a_4\left(\dfrac{T_{\mathrm{s}}}{100}\right) + a_5\left(\dfrac{T_{\mathrm{s}}}{100}\right)^2\right)$		15
	$a_0 = -60.2409,\ a_1 = 93.4517,\ a_2 = 23.3585,\ a_3 = 0.023517,$ $a_4 = -0.023656,\ a_5 = 0.0047036$		

(Continued on the next page)

Supplementary Table 3 (continued)

Process	Function	Unit	Ref.
	$\log K_1 = b_0 + b_1/T_s + b_2 \ln(T_s) + b_3 sal + b_4 sal^2$	mol kg^{-1}	16
	$b_0 = 62.008, b_1 = -3670.7, b_2 = -9.7944, b_3 = 0.0118, b_4 = -1.16\times10^{-4}$		
	$\log K_2 = c_0 + c_1/T_s + c_2 sal + c_3 sal^2$	mol kg^{-1}	16
	$c_0 = -4.777, c_1 = -1394.7, c_2 = 0.0184, c_3 = 1.18\times10^{-4}$		
	$\log K_{sp} = d_0 + d_1 T_s + d_2/T_s + d_3 \ln(T_s) + \left(d_4 + d_5 T_s + d_6/T_s\right)\sqrt{sal} + d_7 sal + d_8 sal^{1.5}$	mol kg^{-1}	17
	$d_0 = -171.9065, d_1 = -0.077993, d_2 = 2839.319, d_3 = 71.595,$ $d_4 = -0.77712, d_5 = 2.8426\times10^{-3}, d_6 = 178.34, d_7 = -0.07711,$ $d_8 = 4.1249\times10^{-3},$		
Subduction into the mantle			
Organic carbon subduction flux			
	$J^{s}_{org} = J^{s,*}_{org}\left(\frac{J^{b}_{org}}{J^{b,*}_{org}}\right) f_G$	mol C yr^{-1}	This study
Carbonate carbon subduction flux			
	$J^{s}_{carb} = J^{s,*}_{carb}\left(\frac{J^{b}_{carb}}{J^{b,*}_{carb}}\right) f_G$	mol C yr^{-1}	This study
Pyrite sulphur subduction flux			
	$J^{s}_{py} = J^{s,*}_{py}\left(\frac{J^{b}_{py}}{J^{b,*}_{py}}\right) f_G$	mol S yr^{-1}	This study
Iron (hydro)oxide subduction flux			
	$J^{s}_{Fe\text{-}ox} = J^{s,*}_{Fe\text{-}ox}\left(\frac{1-DOA}{1-DOA^*}\right) f_G$	mol Fe yr^{-1}	This study

Supplementary Table 4. Parameter values for photochemical parameterization

	fCH$_4$ (ppmv)				
	1	10	100	1000	2000
p_{O2} <10^{-9} bar					
α_0	-5.7265×10^{4}	-4.0362×10^{4}	2.8140×10^{4}	-5.2833×10^{4}	3.3356×10^{4}
α_1	-3.4227×10^{4}	-2.3417×10^{4}	1.6376×10^{4}	-3.0537×10^{4}	1.8811×10^{4}
α_2	-8.5116×10^{3}	-5.6529×10^{3}	3.9580×10^{3}	-7.3352×10^{3}	4.4119×10^{3}
α_3	-1.1266×10^{3}	-7.2655×10^{2}	5.0870×10^{2}	-9.3713×10^{2}	5.5111×10^{2}
α_4	-8.3711×10^{1}	-5.2437×10^{1}	3.6664×10^{1}	-6.7168×10^{1}	3.8674×10^{1}
α_5	-3.3091×10^{0}	-2.0149×10^{0}	1.4050×10^{0}	-2.5612×10^{0}	1.4455×10^{0}
α_6	-5.4366×10^{-2}	-3.2205×10^{-2}	2.2365×10^{-2}	-4.0598×10^{-2}	2.2484×10^{-2}
p_{O2} <10^{-9} –10^{-3} bar					
α_0	-6.0081×10^{0}	-5.1445×10^{1}	-2.3305×10^{1}	6.0832×10^{1}	4.7518×10^{1}
α_1	1.8022×10^{1}	-3.5535×10^{1}	-9.1294×10^{0}	9.9297×10^{1}	8.7219×10^{1}
α_2	9.1391×10^{0}	-1.6387×10^{1}	-7.4827×10^{0}	4.8257×10^{1}	4.4529×10^{1}
α_3	2.1975×10^{0}	-4.0510×10^{0}	-2.8404×10^{0}	1.1727×10^{1}	1.1325×10^{1}
α_4	2.8479×10^{-1}	-5.4278×10^{-1}	-5.1671×10^{-1}	1.5268×10^{0}	1.5394×10^{0}
α_5	1.9048×10^{-2}	-3.7253×10^{-2}	-4.4860×10^{-2}	1.0163×10^{-1}	1.0678×10^{-1}
α_6	5.1560×10^{-4}	-1.0263×10^{-3}	-1.4976×10^{-3}	2.7141×10^{-3}	2.9670×10^{-3}
p_{O2} >10^{-3} bar					
α_0	-2.1503×10^{1}	-2.1539×10^{1}	-2.1856×10^{1}	-2.1878×10^{1}	-2.2065×10^{1}
α_1	-8.4092×10^{-1}	-7.7956×10^{-1}	-9.2312×10^{-1}	-5.1388×10^{-1}	-9.7218×10^{-1}
α_2	1.0188×10^{-3}	-4.4758×10^{-3}	-5.6259×10^{-2}	3.1136×10^{-1}	1.0592×10^{-1}
α_3	-2.2874×10^{-2}	-2.4131×10^{-2}	-3.5599×10^{-2}	3.3290×10^{-2}	2.0702×10^{-3}
α_4	0	0	0	0	0
α_5	0	0	0	0	0
α_6	0	0	0	0	0

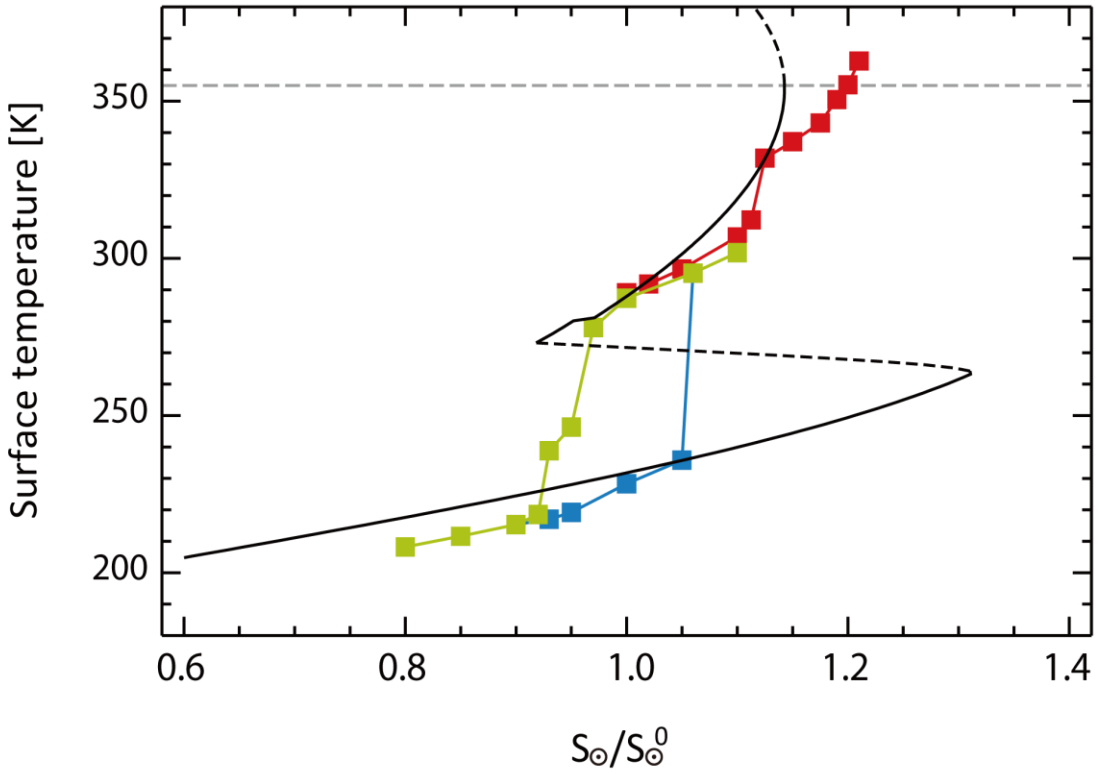

Supplementary Fig. 1. **Surface temperature as a function of the relative stellar flux.** Black line represents the results obtained from an energy balance model used in this study (see Methods), assuming fCO_2 = 280 ppmv and fCH_4 = 0.715 ppmv. Solid and dashed lines represent stable and unstable solutions, respectively. The lines with symbols represent results obtained from a 3-D climate model[13]. Different colour lines represent different initial conditions (red = modern Earth condition with an increasing solar forcing, green = modern Earth condition with a decreasing solar forcing, blue = a globally glaciated state with increasing solar forcing). The horizontal grey dashed line represents the temperature above which diffusion-limited water loss could remove an Earth ocean of water within about 1 Gyr[13].

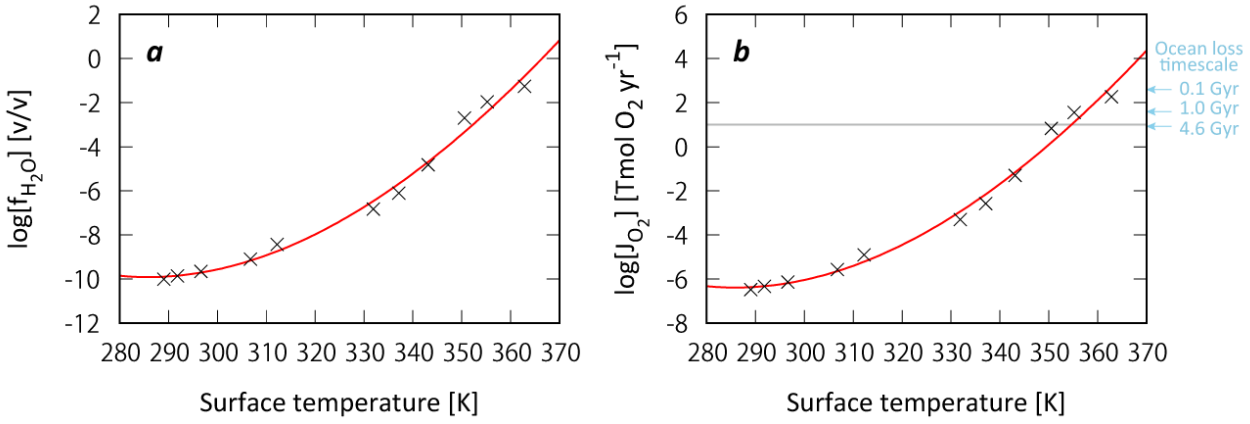

Supplementary Fig. 2. **Empirical relationship between surface temperature and water loss flux to space.** (**a**) The stratospheric water vapour concentration as a function of global average surface temperature. Black crosses show individual GCM results obtained from Wolf et al. (2017)[13], while the red curve shows our polynomial fit. (**b**) Hydrogen escape rate (in terms of an abiotic O_2 flux) as a function of global average surface temperature. The approximate O_2 flux from Earth's modern biosphere is shown by the grey horizontal line. The ocean loss timescales are also represented by blue arrows.

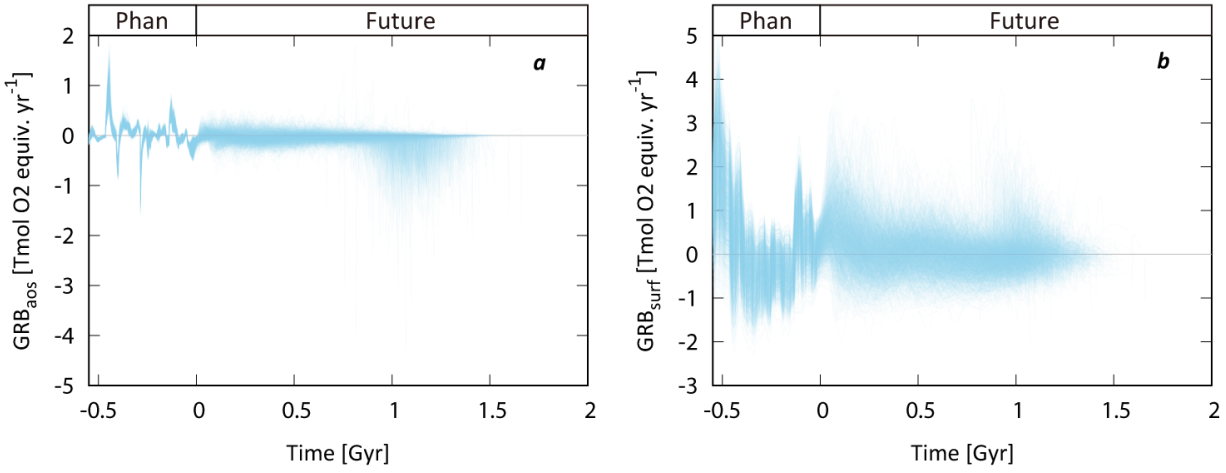

Supplementary Fig. 3. The default Monte Carlo simulations showing the evolution of redox budget. (**a**) The ocean-atmosphere system. (**b**) The exogenic (ocean-atmosphere-crust) system. Positive values denote gaining the oxidizing power.

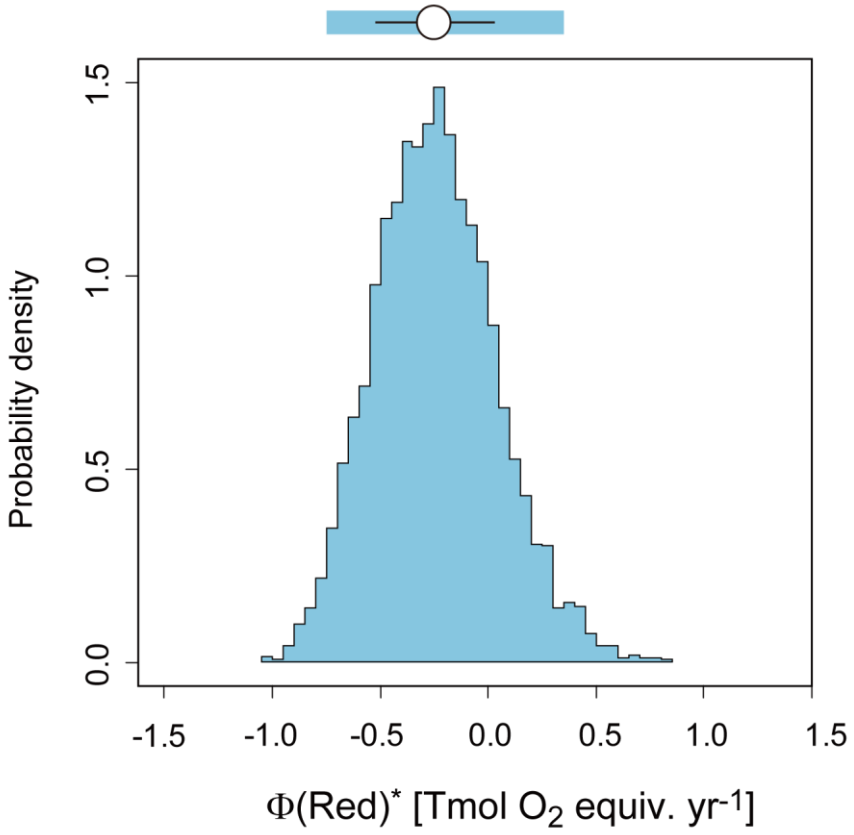

Supplementary Fig. 4. Monte Carlo simulations showing the probability density for the modern values of the net input flux of reducing power from the mantle to the surface system for successful scenarios (*n* = 4,787). Open circle denotes a median value. The error bar and shaded region denote 1σ and 95% credible intervals, respectively.

Supplementary Discussion:

Biogeochemical evolution in response to the secular increase in the solar luminosity. Our default model projections of a long-term decline in atmospheric O_2 (Fig. 2a and Extended Data Figs. 4–8) are accompanied by a series of biogeochemical responses. Our default simulations confirm that atmospheric CO_2 levels predictably decrease with increasing the solar luminosity (Fig. 2c and Extended Data Figs. 4–6), representing a fundamental climate 'thermostat' stabilizing Earth's climate throughout its evolutionary history. Nevertheless, Earth will gradually warm with time in the future (Extended Data Fig. 6c). This can be attributed to the weakening of the negative feedback imposed by the carbonate-silicate cycle due to the drawdown of atmospheric CO_2. Another consequence of atmospheric CO_2 drawdown is a suppression of global biospheric activity (and O_2 production): declining CO_2 reduces the activity level of terrestrial plant productivity, because carbon fixation by land plants is limited by low ambient CO_2 (Extended Data Figs. 1 and 7). Since plant-mediated chemical weathering and associated nutrient (phosphorus) discharge from the crust to the ocean becomes suppressed, the activity level of the marine ecosystem also decreases with time (Extended Data Fig. 7). From the carbon cycle perspective, this 'carbon starvation' mechanism provides stabilizing feedback against further drawdown of atmospheric CO_2 via an increase of the ocean-atmosphere carbon pool. These projections are consistent with previous results[5], with the important difference that in our model CH_4 cycling also contributes to radiative forcing. The drop in atmospheric O_2 leading to oceanic deoxygenation also promotes biospheric CH_4 degassing from the oceans to the atmosphere, resulting in the gradual accumulation of CH_4 in the atmosphere (orange lines in Fig. 2b and Extended Data Figs. 4–6).

Perhaps even more remarkably, the model predicts that the loss of the photosynthetic biosphere leads to a 'great deoxygenation', which leads to an abrupt shift of atmospheric O_2 concentrations to levels reminiscent of the Archean Earth ($<10^{-6}$ PAL) with an attendant increase in CO_2 and CH_4 (Fig. 2 and Extended Data Figs. 4–6). Changes in source/sink fluxes of O_2 are gradual but reach a tipping point at which the O_2 sink flux exceeds the long-term source of O_2 (from the flux of organic carbon and pyrite sulphur burial), allowing O_2 to decrease to a new equilibrium level. Importantly, the deoxygenation is accelerated by positive feedback loops inherent in the Earth system. After the global surface temperature exceeds ~300K, further warming begins to suppress terrestrial and marine biospheric activities (Extended Data Figs. 1 and 7), leading further deoxygenation of the atmosphere. This also tends to increase atmospheric CH_4, which in turn

accelerates surface warming. The atmospheric deoxygenation also stimulates a positive feedback loop among the O_2-O_3-CH_4 photochemical network in response to the loss of a stratospheric ozone layer[6,9] when the atmospheric O_2 concentration reaches a certain threshold (approximately a few % PAL in this model). The loss of the ozone layer results in a collapse of terrestrial productivity due to a sharp increase in harmful UV irradiance in combination with near-starvation of CO_2 and global warming of >5K (from ~310 K to >315 K; Extended Data Figs. 4–6), yielding a severely limited global net primary production (NPP) (a few percent or less of the present value). This diminishes biotic-driven silicate rock weathering and thereby tends to result in an abrupt increase in atmospheric CO_2 (Extended Data Figs. 4–6). Because methane fluxes are still relatively large from poorly oxygenated oceans after the 'great deoxygenation', methane also rises to >10 ppmv, although not to such large concentrations as in the Archaean before the advent of oxygenic photoautotrophs (~10^3 ppmv)[18,19]. Our results imply that the switch of atmospheric redox state to less oxygenation state accelerates the loss of water into space, shortening the lifespan of Earth's aqua planet state than previously thought. However, it is important to note that abiotic O_2 production due to an increase in stratospheric water vapour plays only a minor role in the oxygen budget during the period considered in this study (Supplementary Figs. 2). Testing these predictions quantitatively using 1D photochemistry models should be a fruitful topic for future research aiming at tightening constrains on the ultimate fate of Earth's biosphere. It is also important to note that deoxygenation is further exacerbated because the ocean ecosystem switches to a CO_2-limitation, rather than micronutrients (such as N and P), thereby losing a phosphorus-based stability feedback for regulating atmospheric O_2 (Extended Data Fig. 8). It is generally thought that the phosphorus-mediated coupling of ocean productivity and atmospheric O_2 have acted as a safeguard against catastrophic depletion of atmospheric O_2 (ref.[20]). However, our model predicts that the availability of inorganic carbon (CO_2 and HCO_3^-) will become a limiting factor for marine primary producers in the distant future. As a result of the positive feedbacks that have destabilizing effects on the atmospheric O_2 combined with the loss of negative feedbacks, the Earth system plunges into an anoxic state, with a CO_2-starved biosphere and relatively high surface temperatures.

Supplementary References

1 Bergman, N. M., Lenton, T. M. & Watson, A. J. COPSE: A new model of biogeochemical cycling over Phanerozoic time. *Am. J. Sci.* **304**, 397-437, doi:10.2475/ajs.304.5.397 (2004).

2 Byrne, B. & Goldblatt, C. Radiative forcing at high concentrations of well-mixed greenhouse gases. *Geophys. Res. Lett.* **41**, 152-160, doi:10.1002/2013gl058456 (2014).

3 Lenton, T. M. & Watson, A. J. Redfield revisited: 1. Regulation of nitrate, phosphate, and oxygen in the ocean. *Glob. Biogeochem. Cycles* **14**, 225-248, doi:10.1029/1999gb900065 (2000).

4 Prentice, I. C. *et al.* in *Climate Change 2001: the Scientific Basis* (eds J. T. Houghton *et al.*) Ch. 183-238, (Cambridge University Press, 2001).

5 Caldeira, K. & Kasting, J. F. The life span of the biosphere revisited. *Nature* **360**, 721-723 (1992).

6 Claire, M. W., Catling, D. C. & Zahnle, K. J. Biogeochemical modelling of the rise in atmospheric oxygen. *Geobiology* **4**, 239-269, doi:10.1111/j.1472-4669.2006.00084.x (2006).

7 Lenton, T. M. in *Fire Phenomena and the Earth System* 289-308 (2013).

8 Beerling, D., Berner, R. A., Mackenzie, F. T., Harfoot, M. B. & Pyle, J. A. Methane and the CH_4 related greenhouse effect over the past 400 million years. *Am. J. Sci.* **309**, 97-113, doi:10.2475/02.2009.01 (2009).

9 Goldblatt, C., Lenton, T. M. & Watson, A. J. Bistability of atmospheric oxygen and the Great Oxidation. *Nature* **443**, 683-686, doi:http://www.nature.com/nature/journal/v443/n7112/suppinfo/nature05169_S1.html (2006).

10 Opdyke, B. N. & Wilkinson, B. H. Carbonate mineral saturation state and cratonic limestone accumulation. *Am. J. Sci.* **293**, 217-234, doi:10.2475/ajs.293.3.217 (1993).

11 Lenton, T. M. & Watson, A. J. Redfield revisited: 2. What regulates the oxygen content of the atmosphere? *Glob. Biogeochem. Cycles* **14**, 249-268, doi:10.1029/1999gb900076 (2000).

12 Williams, D. M. & Kasting, J. F. Habitable Planets with High Obliquities. *Icarus* **129**, 254-267, doi:http://dx.doi.org/10.1006/icar.1997.5759 (1997).

13 Wolf, E. T., Shields, A. L., Kopparapu, R. K., Haqq-Misra, J. & Toon, O. B. Constraints on Climate and Habitability for Earth-like Exoplanets Determined from a General Circulation Model. *Astrophys. J.* **837**, 107, doi:10.3847/1538-4357/aa5ffc (2017).

14 Lenton, T. M., Daines, S. J. & Mills, B. J. W. COPSE reloaded: An improved model of biogeochemical cycling over Phanerozoic time. *Earth-Science Reviews* **178**, 1-28, doi:https://doi.org/10.1016/j.earscirev.2017.12.004 (2018).

15 Weiss, R. F. Carbon dioxide in water and seawater: the solubility of a non-ideal gas. *Marine Chemistry* **2**, 203-215, doi:https://doi.org/10.1016/0304-4203(74)90015-2 (1974).

16 Dickson, A. G. & Millero, F. J. A comparison of the equilibrium constants for the dissociation of carbonic acid in seawater media. *Deep Sea Research Part A. Oceanographic Research Papers* **34**, 1733-1743, doi:https://doi.org/10.1016/0198-0149(87)90021-5 (1987).

17 Pilson, M. E. Q. *An Introduction to the Chemistry of the Sea*. 2 edn, (Cambridge University Press, 2012).

18 Kharecha, P., Kasting, J. & Siefert, J. A coupled atmosphere–ecosystem model of the early Archean Earth. *Geobiology* **3**, 53-76, doi:10.1111/j.1472-4669.2005.00049.x (2005).

19 Ozaki, K., Tajika, E., Hong, P. K., Nakagawa, Y. & Reinhard, C. T. Effects of primitive photosynthesis on Earth's early climate system. *Nat. Geosci.* **11**, 55-59, doi:10.1038/s41561-017-0031-2 (2018).

20 Van Cappellen, P. & Ingall, E. D. Redox Stabilization of the Atmosphere and Oceans by Phosphorus-Limited Marine Productivity. *Science* **271**, 493-496, doi:10.1126/science.271.5248.493 (1996).